


Effect of Organoclay and Preparation Method on Properties of Antimicrobial Cellulose Acetate Films

Francisco J. Rodríguez ^{1*}, Romina L. Abarca,¹ Julio E. Bruna,¹ Paula E. Moya,¹ María J. Galotto,¹ Abel Guarda,¹ Marisa Padula²

¹Faculty of Technology, Department of Food Science and Technology, Food Packaging Laboratory (LABEN). Center for the Development of Nanoscience and Nanotechnology (CEDENNA), University of Santiago de Chile, Santiago, Chile

²Packaging Technology Center (CETEA), Institute of Food Technology (ITAL), São Paulo, Brazil

The aim of the present study was oriented to evaluate the effect of a commercial organoclay and the technique of preparation on the physical and antimicrobial properties of active eco-friendly nanocomposites films. To this antimicrobial nanocomposite films were fabricated from cellulose acetate (CA) powder, triethyl citrate (TEC) plasticizer, a commercial organoclay Cloisite30B (C30B), and cinnamaldehyde (Ci) as active agent. All nanocomposites showed the intercalation of the polysaccharide inside the organoclay structure, however, the level of the intercalation and the quality of the clay dispersion were dependent on the method selected to prepare them (solution-casting or extrusion). In addition, nanocomposites obtained by extrusion evidenced a better dispersion of organoclay. Important changes on the color properties of films were evidenced, which was associated to the thermal degradation of the quaternary ammonium surfactant of the Cloisite30B. On the other hand, organoclay was unable to reduce the cinnamaldehyde loss during the extrusion and storage, nevertheless, a slight effect of the Cloisite30B on the cinnamaldehyde release to a food simulant was observed to nanocomposites prepared by extrusion. Finally, despite cinnamaldehyde loss was observed over time, the content of residual active compound into the films was able to impart antimicrobial activity against *Escherichia coli* for 14 weeks. POLYM. COMPOS., 40:2311–2319, 2019. © 2018 Society of Plastics Engineers

INTRODUCTION

Currently, a large number of industries are consumers of fossil-based plastic (e.g., polyolefins). These plastic materials

have excellent physical properties with a wide range of applications that are also low cost and easy processing materials. Although these materials offer many advantages, their wastes have accumulated in massive proportions, which have had a negative impact on the environment [1]. So, plastics have become a major threat to the environment because of their poor biodegradability and a high visibility in the waste stream. Therefore, these problems are exacerbated by there is lack of efficient end of life management of plastic waste, hence the life cycle of plastic materials ends at waste disposal facilities [2]. In this context, the food industry has been identified as one of the highest consumers of petroleum-based plastic materials, such as polyolefins (polyethylene – PE, polypropylene – PP), polystyrene (PS), polyethylene terephthalate (PET), polyvinyl chloride (PVC), and polyamides (PA), which are the most used by the industry [3].

Different strategies have been proposed to reduce the environmental impact of waste plastics, such as reducing the weight of packaging and the use of biodegradable, recyclable, and/or compostable packaging materials. Bio-based polymers extracted from biomass or synthesized from monomers derived from biomass is an approach that can be applied in food industry, particularly considering that most of them are obtained from renewable resources and in some cases they are also biodegradable [4]. Despite the environmental benefits of these materials, they do not present the required properties for food packaging, due to some physical properties, such as high permeability, poor mechanical properties, among others. Different strategies have been proposed to overcome this predicament, and among them nanotechnology approach would improve some of the film properties to make these polymers more like the traditional polymer materials [5].

Polymer nanocomposites are heterogeneous systems. They consisted of a polymer matrix reinforced with filler that has at least one dimension under 100 nm. These nanofillers can

Correspondence to: Francisco J. Rodríguez; e-mail: francisco.rodriguez.m@usach.cl

Contract grant sponsor: Comisión Nacional de Investigación Científica y Tecnológica; contract grant number: FB0807. contract grant sponsor: Universidad de Santiago de Chile; contract grant numbers: USA 1555 - VRI-DEI 081771RM MOV; USA 1555 - VRI-DEI 081771RM_MOV. DOI 10.1002/pc.25041

Published online in Wiley Online Library (wileyonlinelibrary.com).

© 2018 Society of Plastics Engineers

be one-dimensional (e.g., nanofibers), two-dimensional (e.g., clays), or three-dimensional (e.g., nanosilver). Uniform dispersion of some nano-sized fillers produce systems with a high aspect ratio. Presence of a significant interfacial area and the nanoscale of these fillers essentially differentiate polymer nanostructured composites from conventional filled plastics and composites. So, the physical properties (barrier, thermal, optical, magnetic, and electric) of polymeric materials are significantly modified when low feed of nanofillers are used (<5 wt%). Regarding to nanofillers, clays have been considered as fundamental fillers to develop nanocomposite materials oriented to the food packaging industry because they can reduce the oxygen and water vapor diffusion through plastic materials [6,7]. The effect of clay dispersion on the gas permeability properties for nanocomposites has been reported by different authors [8–14]. In addition, these studies have also reported the need to modify the clay structure with quaternary ammonium with long alkyl chains to produce organoclays which favors the nanoparticle-polymer interaction to produce nanocomposites [15,16].

In last decades, studies based on nanocomposites have been mainly focused on the development of materials based on traditional polymers. However, the use of bio-based polymers to produce bio-nanocomposites is a new area. The most studied bio-nanocomposites suitable for packaging applications are starch and cellulose derivatives, polylactic acid (PLA), polycaprolactone (PCL), poly(butylene succinate) (PBS), and polyhydroxybutyrate (PHB) [17]. Considering cellulose as the most abundant natural polymer, its application in the plastics industry is an attractive substitute for traditional plastics. Studies applied to cellulose are focused on cellulose derivatives because they present better processability than pure cellulose. Chemical modification on the cellulose structure reduces the formation of hydrogen bond into the structure of cellulose because the –OH groups are blocked by the presence of different substituents [18]. Within cellulosic derivatives, cellulose acetate (CA) and cellulose acetate butyrate (CAB) are of particular interest because they are biodegradable polymers and have excellent optical clarity and high toughness; therefore, these cellulose derivatives can be processed by melting and solubilized in different solvents. To improve the processability of cellulose derivatives, different authors have reported the use of triethyl citrate (TEC) as nontoxic plasticizer agent [19–22].

On the other hand, the concept of food packaging has changed from a passive system, which acts as a simple container and/or insulating barrier from the outside environment, to active packaging that absorbs or release substances which interact with food, increasing the food's shelf life and quality [23–25]. For this reason, active food packaging has experienced a remarkable growth in recent years. The uses of bio-based polymers have risen to be an important alternative to produce active materials. In this way, development of eco-materials with special functionalities such as antimicrobial or antioxidant activities could be transcendental to the promotion of new active food packaging.

To develop antimicrobial food packaging, different types of antimicrobial agents have been used, however, it can be highlighted the use of essential oil derivatives. Essential oils and their constituents are categorized as GRAS (Generally Recognized as Safe) by the US Food and Drug Administration. For this reason, essential oils (EOs) have been used as antimicrobial, antifungal, and antioxidant agents [26]. Moreover, the use of active antimicrobial materials for food packaging could lead to the reduction or total absence of the preservatives content in the food. Thus, the consumer will have access to more natural products, especially if the preservative also has a natural origin, such as essential oil derivative [27]. Regarding to EOs derivatives, cinnamaldehyde (3-phenyl-2-propenal) is a major component of cinnamon and cassia oils. This aldehyde has shown an important effect on the growth of yeast, bacteria, and molds [28,29]. As a result, cinnamaldehyde has been incorporated into different materials to produce antimicrobial packaging [30–34]. Several studies have shown the antimicrobial effectivity of active films based on cinnamaldehyde; however, studies oriented to evaluate the antimicrobial capacity over the time are limited. This is particularly important due to the highly volatile nature of this kind of compound. Regarding to this issue, clay dispersion level into nanocomposites could be the key to design active materials based on EOs derivatives where it is necessary to reduce the volatilization of the active agent according to the tortuous complex pathway generation used to explain the reduction of the gas permeability in nanocomposite films. In this way, the method of preparation of the nanocomposite films must also be considered because the clay dispersion can be affected by the method selected.

Based on the above, the aim of the present study was to evaluate the effect of the commercial organoclay (Cloisite30B) and technique of preparation of active cellulose acetate films on the physical properties of CA films, and cinnamaldehyde loss, and antimicrobial activity against *Escherichia coli* during 14 weeks.

EXPERIMENTAL

Materials and chemicals

The commercial organoclay Cloisite30B (C30B), a clay modified with methyl, tallow (~65% C₁₈, ~30% C₁₆, and ~C₁₄), bis-2-hidroxyethyl, quaternary ammonium chloride, was provided by Southern Clay Products, Inc. (Gonzalez, TX). Cellulose acetate (39.8% w/w acetyl content with an average molecular weight of about 30,000 Da), triethyl citrate (>99%) and cinnamaldehyde (99%) were supplied by Aldrich (St. Louis, MO). Sodium dihydrogen orthophosphate (NaH₂PO₄·H₂O) was supplied by Merck (Darmstadt, Germany); disodium hydrogen orthophosphate (Na₂HPO₄·2H₂O) was supplied by J.T. Baker (Edo. De Méx., México). Neutralized bacteriological peptone was supplied from Oxoid (Hampshire, England); peptone from casein and agar-agar,

methanol, ethanol, and acetonitrile HPLC grade were supplied by Merck. Acetone (technical grade) was supplied by Soviquim (Santiago, Chile).

Cellulose acetate nanocomposite films preparation by casting solution technique (CT)

The nanocomposites were prepared according to a procedure previously reported [35]. The selection of the composition of the nanocomposites was based on previous studies [1, 19, 42, 54]. Accordingly, nanocomposite films consisted of 5 wt% of C30B, 20 wt% of TEC, and 2 wt% of cinnamaldehyde (CA/TEC/C30B/Ci). Nanocomposites were prepared by means of a casting technique using acetone as a solvent. 10 g of CA, 2.4 mL of TEC, and 0.51 mL of cinnamaldehyde were dissolved in 150 mL of acetone under vigorous stirring for 1 h at room temperature (RT). In parallel, 0.68 g of C30B was dispersed in 50 mL of acetone and sonicated for 30 min at RT. Later, the CA solution was added to the organoclay suspension under vigorous stirring, and this mixture was stirred for 60 min at RT. Afterward, 80 mL of mixture was added to a Petri dish ($\phi = 20$ cm) and dried at 40°C in an oven for 4 h. Finally, the films were removed from the glass disc and stored in polyethylene bags to avoid contamination. As control films, other films based on CA were prepared (CA/TEC, CA/TEC/Ci, and CA/TEC/C30B).

Cellulose acetate nanocomposite films preparation by melt-compounding technique (MT)

At first, CA, TEC (20 wt%), Cloisite30B (5 wt%), and cinnamaldehyde (2 wt%) were mixed manually in a stainless steel container to obtain a homogenous mixture. After that the mixture was melt-extruded through a 20 mm corotating laboratory twin-screw extruder Labtech LTE20 (Samutprakarn, Thailand). The temperature profile of extruder was kept between 180°C and 220°C with die temperature of 220°C. The screw speed was fixed at 70 rpm and the feed at 50 rpm, and the films were collected in a chill roll attachment Labtech LBCR-150 (Samutprakarn, Thailand) at 3 rpm. Finally, the films were stored in polyethylene bags to avoid contamination. CA/TEC, CA/TEC/Ci and CA/TEC/C30B films were also prepared according to the last procedure (section Cellulose acetate nanocomposite films preparation by casting solution technique (CT)).

Cellulose acetate nanocomposite films characterization

Morphology and structure

XRD analysis was carried out in a Siemens Diffractometer D5000 (30 mA and 40 kv) using CuK α ($\lambda = 1.54$ Å) radiation at RT. All scans were performed in a 2θ range 2–10° at 0.02°seg⁻¹. Interlaminar distances were calculated using Bragg's law [36]. On the other hand, to TEM analysis ultrathin (50–60 nm) sections were cut using a Sorvall MT-

IIB ultra-microtome and placed on a copper grid (300 mesh). Samples were examined under a Phillips Tecnai 12 Bio Twin TEM at 80 kV. Images were recorded using a CCD camera Olympus Megaview G2. Finally, film color was measured using a colorimeter Minolta Chroma Meter (CR 410, Japan). The CIELAB scale was used, and lightness (L^*) and chromaticity parameters a^* (red–green) and b^* (yellow–blue) were measured. A white standard color plate ($L^* = 97.11$, $a^* = -0.03$, and $b^* = 1.96$) was used as the background for color measurements, and D65 illuminant and to evaluate changes on the color of films 2° observer were used for analyses. Each analysis was performed in 20 replicates, and the average values were reported in the results. Color differences (ΔE) were calculated using the equation $\Delta E = [(\Delta L^*)^2 + (\Delta a^*)^2 + (\Delta b^*)^2]^{1/2}$.

Cinnamaldehyde content

The content of cinnamaldehyde from CA and CA nanocomposite films were tracked for 14 weeks and its quantification was performed by high performance liquid chromatography (HPLC). To determine the content of active compound a solid–liquid extraction was performed. To this, 0.005 g of film was introduced into a 50 mL volumetric flask and then 46 mL of methanol was added into this. Afterwards, the stoppered flask was placed inside of Elmasonic S10H ultrasonic bath (Singen, Germany) with a frequency of 37 kHz for 10 min at room temperature. Subsequently, 5 mL of sample was taken from the volumetric flask using a syringe, and then this sample was filtered through a 0.45 μm membrane filter (Millipore). Finally, 1 mL of the filtered sample was placed into a 1 mL flask to the chromatographic analysis.

The quantification of cinnamaldehyde was according to the method described by Dighe et al. [37], with some modifications. Chromatographic analysis was performed in a Hitachi LaChron Elite chromatograph (Darmstadt, Germany) equipped with a Hitachi L-2455 diode array detector, a Hitachi L-2200 autosampler and a C-18 Lichrospher column (250 \times 4.6 mm, i.d). The mobile phase consisted of a mixture of distilled water:acetonitrile:methanol (55:35:10) at a flow rate of 1.0 mL min⁻¹, and the detection of cinnamaldehyde was carried out at 283 nm. The injection volume was 5 μL and the oven temperature was constant at 35°C. Quantification of the active compound was carried out by comparison of the chromatographic peak areas with standards in the same concentration range. Calibration curve was run at eight concentrations from 0.01 to 40 ppm using appropriately diluted standards of cinnamaldehyde in methanol.

Cinnamaldehyde release kinetics

Active cellulose acetate films (1 dm²) were immersed in glass tubes with 130 mL of ethanol solution (10% v/v) as food simulant (Regulation (EU)N°10/2011). The samples were placed on metal supports inside the tubes in a way that the film did not touch the wall of the glass tubes. The

glass tubes were kept in an oven at 40°C. To obtain the cinnamaldehyde concentration evolution in the simulant as a time function, the food simulant samples were collected (1 mL) at different times for further HPLC analysis. Each data shown is the average value of three replicates.

Antimicrobial activity

The antimicrobial activity of CA and CA nanocomposites films against *E. coli* ATCC 25922 was based on the ASTM E2149–13 standard [38] with modifications, which is a quantitative antimicrobial test method performed under dynamic contact conditions.

A preinoculum was prepared by transferring bacterial colonies with a handle loop in a test tube with 5 mL of *Luria Bertani* (LB) broth. The test tube was incubated for 16 h at 3°C and constant agitation at 150 rpm. After this time, 1 mL of the bacterial suspension was taken and transferred to a test tube with 15 mL of LB medium to obtain inoculum. It was incubated at 37°C in a shaking incubator at a speed of 150 rpm, until the culture was found in the range 0.6–0.8 optical density measurements, which was carried out at different times in a UV–vis Shimadzu UV-1700 spectrophotometer (Kyoto, Japan) at 600 nm. This range ensures that the bacterial cells are in exponential phase and fresh. Subsequently, diluting fixed concentration prepares work of 5×10^6 UFC mL⁻¹ of the microorganism in a phosphate buffer stock solution of KH₂PO₄ 0.3 mM (pH 6.8).

Film samples were cut into small pieces, weighed (approximately 0.5 g), which were previously sterilized with ultraviolet light for 2 min, and then placed into test tubes containing 10 mL of phosphate buffer stock solution

(5×10^6 UFC mL⁻¹). After that, the tubes were incubated with stirring at 150 rpm and 37°C for a period of 24 h. After the incubation 1:10 serial dilutions (900 µL of phosphate buffer and 100 µL of culture in dynamic contact) from –1 to –5 dilutions were performed, which were seeded by the technique of microdroplets in triplicate. Once microdroplets were dried, the plates were incubated at 37°C for 16 h. Finally, the colonies were counted, and the antimicrobial activity expressed as log₁₀ bacteria reduction.

RESULTS AND DISCUSSION

Morphology and structure

In order to evaluate the interaction between the polymer and organoclay, a XRD analysis was performed. Figure 1 shows the XRD patterns of Cloisite 30B, CA/TEC, CA/TEC/C30B, and CA/TEC/C30B/Ci films obtained by solution-casting (left) and extrusion techniques (right), respectively. All nanocomposites demonstrated intercalation of the polymer into the structure of organoclay, which is evidenced by the displacement of d₀₀₁ peak of Cloisite30B to lower 2θ values.

The intercalation level depended on the technique used to prepare the different films. It is possible to observe that nanocomposites prepared by CT technique showed a higher intercalation of the polymer in the organoclay structure than those prepared by MT technique. Indeed, these nanocomposites showed a broader diffraction peak than the obtained by extrusion process. These results could agree with a heterogeneous intercalation of the CA into the Cloisite30B structure that has been previously reported for organoclays based on

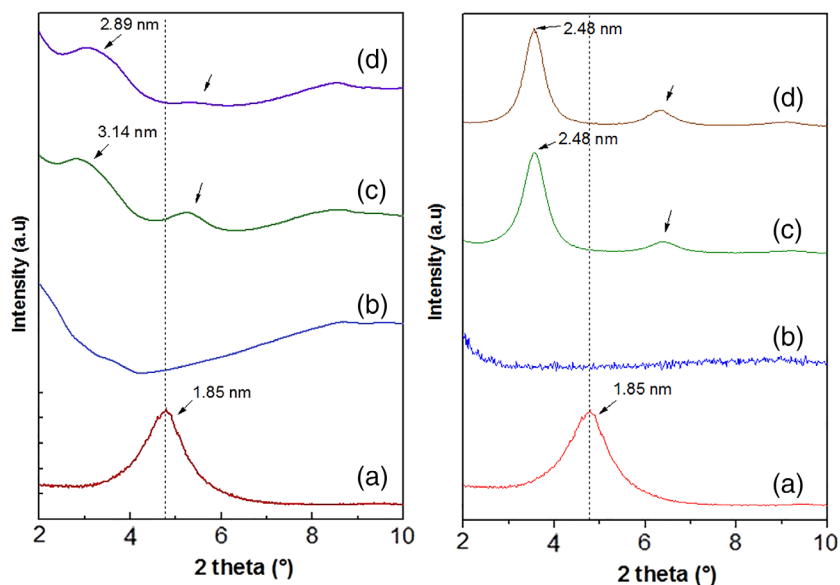


FIG. 1. X-ray diffraction (XRD) patterns of (a) Cloisite 30B, (b) CA/TEC, (c) CA/TEC/C30B; and (d) CA/TEC/C30B/Ci. Left: films obtained by CT method. Right: films obtained by MT method. [Color figure can be viewed at wileyonlinelibrary.com]

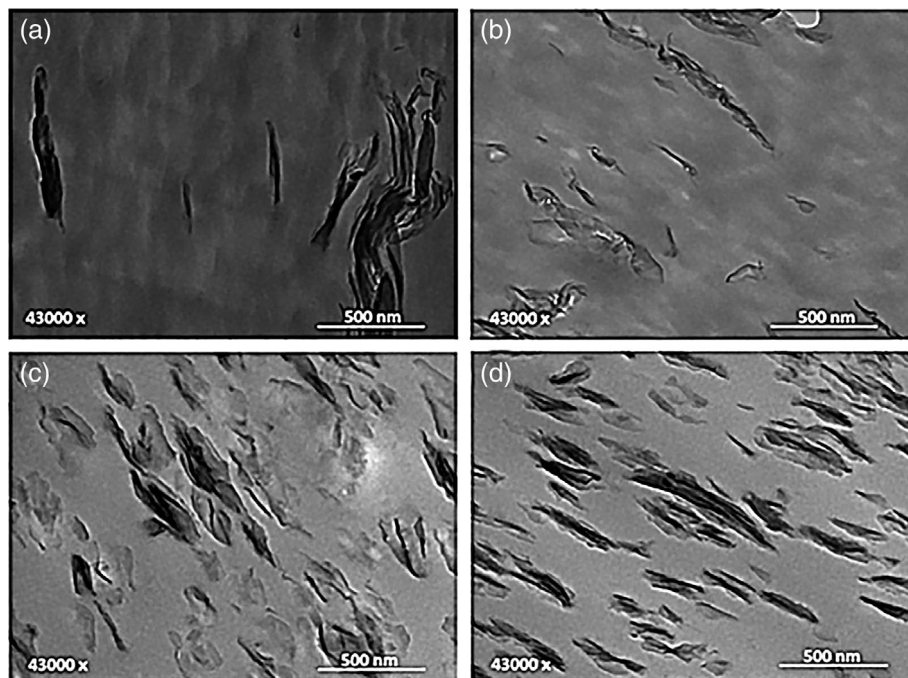


FIG. 2. TEM images of (a) CT CA/TEC/C30B; (b) CT CA/TEC/C30B/Ci; (c) MT CA/TEC/C30B; (d) MT CA/TEC/C30B/Ci.

montmorillonite and chitosan [36]. Additionally, CA nanocomposites obtained by MT technique showed a sharp diffraction d_{001} peak, which agrees with a homogeneous intercalation of CA in the layered structure of the organoclay. Furthermore, XRD patterns to all nanocomposites show diffraction peaks to higher values of $2\theta = 4.78^\circ$ and nanocomposites obtained by CT technique showed a peak around 5.25° while those obtained by MT showed a peak around 6.38° . Presence of these peaks could be explained by certain solubility of the ammonium component (*methyl, tallow, bi-2-hydroxyethyl, quaternary ammonium*). It belongs to the commercial organoclay in acetone to films based on solving-casting, and the degradation of this ammonium component by high temperatures when the nanocomposite films are prepared by extrusion.

As a result, the presence of a residual organoclay characterized by a smaller interlaminal distance due to the organic ammonium component loss can be evidenced.

To confirm the result of XRD analysis, a microscopic analysis was performed. Figure 2 summarizes the TEM images of CA/TEC/C30B and CA/TEC/C30B/Ci nanocomposite films obtained by solving-casting and extrusion. Important differences can be observed when preparation techniques are compared. Nanocomposites prepared by solving-casting technique showed a heterogeneous dispersion, which is characterized by presence of organoclay particles in different sizes. In contrast, nanocomposites obtained by extrusion evidenced a better dispersion of organoclay. These nanocomposites were characterized by uniform dispersion where tactoid and intercalated structures were evidenced.

Interestingly, an organoclay orientation can be observed to these nanocomposites. It has been explained that this behavior is favored when the melt of polymeric material and clay filler have a suitable residence time within the extruder that favors clay platelets orient toward the flow direction [39].

With equal importance, optical properties are an essential parameter in the development of new packaging materials. For this reason, the color of the different films was determined using the CIELab scale. Tables 1 and 2 show the color parameters determined by this technique. Significant changes can be observed when Cloisite30B is included in the films, however, these changes were more important in the case of films obtained by the extrusion technique. In contrast, a dark color is observed in the CA/TEC/C30B and CA/TEC/C30B/Ci films. It is well-known that minerals like clays and zeolites, within others, affect the optical properties of plastic materials. However, the changes observed to extruded films were substantial, in relation with the high values of ΔE parameter to nanocomposite films (>7). These high values of ΔE greatly exceed the limit to become perceptible [40]. Color development in the case of nanocomposite films could be caused by a thermal degradation of the quaternary ammonium component from Cloisite30B [41]. The thermal degradation of organoclays has been evidenced in previous studies where nanocomposite films have been elaborated by means of an extrusion process [42,43]. These color changes are negative in terms of application of the nanocomposite films obtained by extrusion because the optical properties of a packaging material are fundamental for selection purposes.

TABLE 1. Color parameters of the films produced by CT.

Sample	L*	a*	b*	ΔE
CA/TEC	97.7 ± 0.27 ^a	-0.07 ± 0.02 ^a	2.18 ± 0.07 ^a	
CA/TEC/C30B	96.9 ± 0.34 ^b	-0.59 ± 0.06 ^b	4.77 ± 0.26 ^b	2.82 ± 0.35 ^a
CA/TEC/Ci	98.1 ± 0.34 ^a	-0.09 ± 0.02 ^a	2.22 ± 0.04 ^a	0.34 ± 0.17 ^b
CA/TEC/C30B/Ci	97.2 ± 0.23 ^c	-0.56 ± 0.03 ^c	4.53 ± 0.12 ^c	2.50 ± 0.16 ^c

Each value is the mean of 10 replicates with the respective standard deviation. Different letters in each column indicate that they are statistically different ($p > .05$) in Fisher applying multiple range test.

TABLE 2. Color parameters of the films produced by MT.

Sample	L*	a*	b*	ΔE
CA/TEC	97.7 ± 0.42 ^a	-0.06 ± 0.01 ^a	2.53 ± 0.16 ^a	
CA/TEC/C30B	93.8 ± 0.59 ^b	-0.13 ± 0.02 ^{a,b}	4.66 ± 0.69 ^b	7.27 ± 0.85 ^a
CA/TEC/Ci	97.9 ± 0.42 ^a	-0.29 ± 0.02 ^b	3.47 ± 0.15 ^c	1.06 ± 0.18 ^b
CA/TEC/C30B/Ci	92.1 ± 0.48 ^c	0.02 ± 0.03 ^c	10.9 ± 0.34 ^d	10.07 ± 0.50 ^c

Each value is the mean of 10 replicates with the respective standard deviation. Different letters in each column indicate that they are statistically different ($p > .05$) in Fisher applying multiple range test.

Cinnamaldehyde content

Table 3 summarizes the results of the evolution of the cinnamaldehyde content into the films obtained by CT and MT techniques during 14 weeks.

A minimal loss of the active compounds can be observed during the first week in the films obtained by CT technique. Nevertheless, an important reduction of the cinnamaldehyde was observed ($\approx 25\%$) in the films obtained by extrusion process. This reduction can be explained by the use of high temperatures ($\approx 200^\circ\text{C}$) to produce the nanocomposite films, which favors the evaporation of the cinnamaldehyde. The evaporation loss of EOs derivatives in extrusion process is a disadvantage of this kind of compounds when they are incorporated by this technique [44]. In this regard, several studies have reported high levels of essential oils derivatives loss during processing. First, a study reported a loss of 28% for thymol, and 39% for linalool to extruded films based on low density polyethylene (LDPE), polyethylene glycol, ethylene vinyl acetate, and those EOs derivatives [45]. Second, Galotto et al. reported a thymol loss of 70% when thymol was extruded with polyethylene [46]. In this study, the effect of temperature and low chemical affinity between the polymer matrix and

the thymol were used to explain this high reduction of the essential oil derivatives into the plastic film. Actually, a loss of more than 90% was reported by Suppakul et al. when they extruded LDPE with linalool or methylchavicol [47]. The same authors reported that the use of a blend of LDPE-ethylene vinyl acetate was able to increase the retention of the active additives into this polymer matrix ($\approx 20\%$). The increase of the essential oil derivatives in the polymer mixture was attributed to the lower processing temperature and a better interaction between the active agents and the polymeric blend. Other strategy to reduce the essential oils derivatives loss can be oriented to increase the tortuous path into the polymer matrix. In consequence, the introduction of clay structures into the cellulose acetate could reduce the evaporation of the active compound. Nevertheless, the effect of the Cloisite30B on the cinnamaldehyde loss during the elaboration processes (CT and MT) was not evidenced in this study, because it was not possible to observe differences in the cinnamaldehyde content between the CA films elaborated with or without the nanofillers during the 14 weeks. Due to all nanocomposites evidenced intercalated structures, as described above, they were not able to produce an important tortuous path that proved to make difficult the diffusion of the cinnamaldehyde thorough the CA matrix, which could be explain if the C30B would have been exfoliated [19]. Interestingly, cinnamaldehyde loss was higher in CT films than MT films during the storage for 14 days. Thus, in CT films it was observed a reduction of cinnamaldehyde content of 28.1% and 27.1% to CA/TEC/Ci and CA/TEC/C30B/Ci, respectively. Therefore, it can be evidenced that the presence of C30B was no able to reduce the cinnamaldehyde loss. On the other hand, in MT films it can be observed a loss of 10.7% and 8.72% to CA/TEC/Ci and CA/TEC/C30B/Ci, respectively. These results show that the technique to prepare the CA films would be a

TABLE 3. Quantification of cinnamaldehyde in the films obtained by CT and MT.

Time (week)	Cinnamaldehyde (wt%)			
	CT		MT	
	CA/TEC/Ci	CA/TEC/C30B/Ci	CA/TEC/Ci	CA/TEC/C30B/Ci
1	1.99 ± 0.26	1.99 ± 0.23	1.49 ± 0.19	1.49 ± 0.10
7	1.74 ± 0.24	1.79 ± 0.21	1.43 ± 0.08	1.47 ± 0.09
14	1.43 ± 0.18	1.45 ± 0.05	1.33 ± 0.07	1.36 ± 0.07

determining factor in the active compound loss. Regarding this, changes on the morphology of the films must be considered. To complement these results, a previous work reported differences in morphology of cellulose acetate films when they were prepared by different techniques (solution-casting method and extrusion process) [48]. In this study, films prepared by solution-casting methods showed more porous films than those prepared by extrusion process (Fig. 3). As a result, the release of cinnamaldehyde from CT films would be more favored than MT films. An effect of the morphology of films was also used to explain the differences of the lysozyme release from active CA films. Indeed, porous films showed higher antimicrobial activity than dense films, which were according to a highest release rate of lysozyme from porous CA films [49].

Cinnamaldehyde release kinetic

It is well-known that the effectiveness of active films is determined in part by the release of active compounds. Thus, it is necessary to control the amount and the rate in which the active compound is released from the active material to the foodstuff.

Figure 4 shows the experimental results of amount of cinnamaldehyde released into ethanol solution (10%) versus time. It can be observed that the equilibrium in the cinnamaldehyde release curves for active cellulose acetate films is reached around 7.7 and 5.6 h of the test for CT and MT films, respectively. As a result, MT films leads to a faster cinnamaldehyde release kinetic than CT films. The observed differences could be explained by the differences in the films thickness. The films thicknesses were $125 \pm 1.32 \mu\text{m}$ and $88.9 \pm 9.43 \mu\text{m}$ for CT and MT films, respectively. These differences would affect the release rate of cinnamaldehyde from active films, which depends on the thickness of the film as it has been reported in other studies based on active films [50]. Therefore, the data show that the highest equilibrium quantity of cinnamaldehyde is released from CT (≈ 150 ppm) films, which is in accordance with the higher

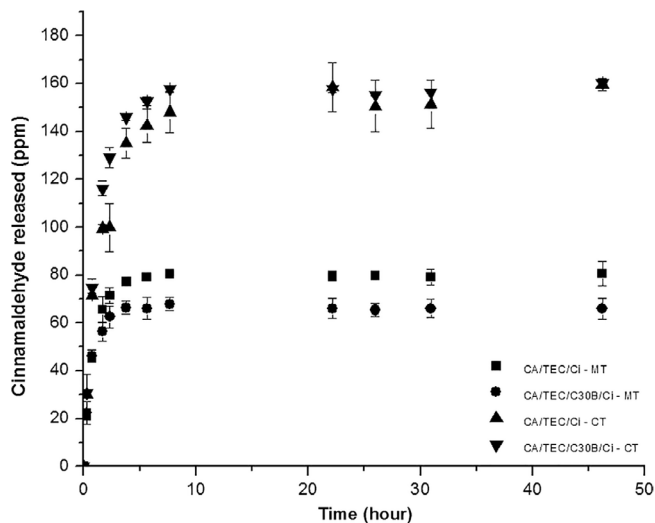


FIG. 4. Amount of cinnamaldehyde release from different active cellulose acetate films plotted in function of time.

initial cinnamaldehyde content observed in CT films in comparison with MT films. Additionally, it was noted that the presence of C30B in CT films was not able to affect the cinnamaldehyde release from the active films. Nevertheless, a slight effect of the C30B can be noticed in MT films. As a result, it can be observed a lower equilibrium quantity of cinnamaldehyde to CA/TEC/C30B/Ci than CA/TEC/Ci. Presence of C30B would favor a chemical interaction with the cinnamaldehyde into the nanocomposite film, which would decrease the content of the active compound that migrate to the food simulant. Thus, results suggest that the presence of C30B and its dispersion into the films would be relevant to control the equilibrium of the active compound between the films and the food simulant.

Antimicrobial activity

The antimicrobial activity of different films was tested against *E. coli* at 1, 7, and 14 weeks (Table 4). It is

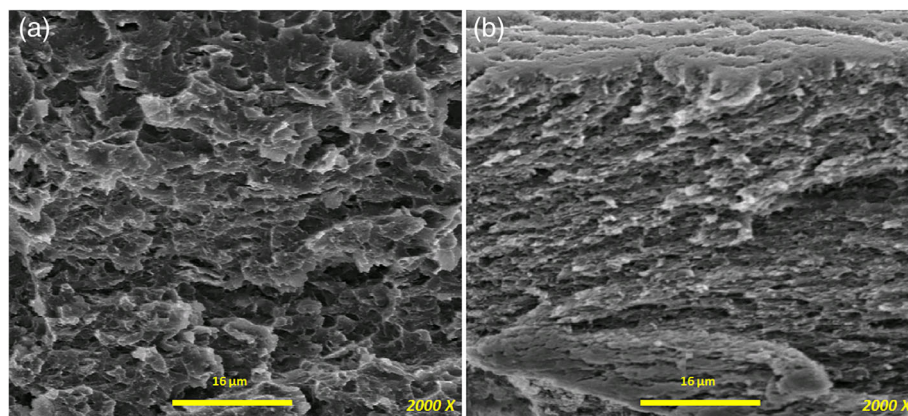


FIG. 3. SEM micrographs for the cross section of the active cellulose acetate nanocomposite films. (a) CA/TEC/C30B/Ci obtained by CT, and (b) CA/TEC/C30B/Ci obtained by MT [48]. [Color figure can be viewed at wileyonlinelibrary.com]

TABLE 4. Representative log reduction in bacterial growth after exposure to CT and MT films at different times.

Time (week)	Log reduction			
	CA/TEC/Ci - CT	CA/TEC/C30B/Ci CT	CA/TEC/Ci - MT	CA/TEC/C30B/Ci MT
1	4.89 ± 0.02	4.68 ± 0.04	5.12 ± 0.04	5.06 ± 0.06
7	2.08 ± 0.11	2.00 ± 0.16	3.72 ± 0.41	3.47 ± 0.12
14	4.09 ± 0.04	4.19 ± 0.19	3.96 ± 0.25	4.21 ± 0.58

important to notice that the antimicrobial action of cinnamaldehyde against *E. coli* was only observed in films with this EOs derivative. After the first week, the growth of *E. coli* was reduced by about 5 log cycles for the active films obtained by CT and MT techniques. This high antibacterial activity was in accordance with the high content of cinnamaldehyde in the films, which was above the minimal inhibitory concentration of this active compound to *E. coli* [29,51]. Afterward, a reduction of the antimicrobial activity is observed, which was in accordance with the cinnamaldehyde loss. Despite the decrease in the content of cinnamaldehyde in the films, the content of this was above the minimum inhibitory concentration (MIC). So, at 7 week of storage, CT films were able to reduce the bacterial population by around 2 log cycles, while for MT films the reduction was around 3.5 log cycles. Interestingly, at 14 weeks the CT and MT showed an increase of the antimicrobial activity. After 14 weeks the diffusion of the cinnamaldehyde from the internal to the surface of the film would favor an increase of the local concentration of the active compound, what would increase its action on the bacterium. In addition, a degradation of CA would also favor the release of the cinnamaldehyde from the different materials. It is well-known that CA can be degraded by a photo-chemical process where formation of radicals initiated by the absorption of light [52]. Moreover, presence of acetic acid as degradation product from deacetylation reaction of CA could also contribute to increase the antimicrobial activity after 14 weeks [35].

CONCLUSIONS

Nanocomposites based on cellulose acetate, Cloisite30B, triethyl citrate, and cinnamaldehyde were prepared using solution-casting and extrusion techniques. Results of XRD evidenced the existence of intercalated nanocomposites; however, the dispersion of the organoclay was favored when the films were obtained by extrusion process. In addition, the extrusion process favored the thermal degradation of the commercial organoclay and an important loss of cinnamaldehyde ($\approx 25\%$). Despite this loss level, the retention of active compound was higher than other studies reported, which was favored for the good affinity between cellulose acetate and cinnamaldehyde. In addition, it was observed than presence of C30B in MT films was unable to reduce the loss of cinnamaldehyde; nevertheless, this organoclay

affected the equilibrium quantity of cinnamaldehyde into a food simulant when release kinetic was performed. Additionally, MT films leads to a faster cinnamaldehyde release kinetic than CT films which was according with differences in the thickness and morphology of these films. A decrease of the cinnamaldehyde content was observed during 14 weeks in all active cellulose acetate films. In spite of this, the active films showed antimicrobial activity against *E. coli* during 14 weeks. In summary, the results obtained in the present study are promising to be applied in the manufacture of eco-friendly active food packaging materials.

ACKNOWLEDGMENTS

The authors are grateful to the National Commission for Scientific and Technological Research, CONICYT, for its financial support from Center of Excellence with Basal Financing, Grant FB0807 (CEDENNA). Finally, the authors thank Universidad de Santiago de Chile for its support (Grant USA 1555 – VRIDEI 081771RM_MOV).

REFERENCES

1. F.J. Rodríguez, A. Coloma, M.J. Galotto, A. Guarda, and J. E. Bruna, *Polym. Degrad. Stab.*, **97** 1996 (2012).
2. A.K. Panda, R.K. Singh, and D.K. Mishra, *Renew. Sustainable Energy Rev.*, **14** 233 (2010).
3. K. Marsh and B. Bugusu, *J. Food Sci.*, **72** R39 (2007).
4. F. J. Rodríguez, M. J. Galotto, A. Guarda, and J. E. Bruna, Modification of cellulose acetate films, K. G. Ramawat, M. R. Ahuj, Switzerland, 219 (2016).
5. S. Ray and M. Okamoto, *Prog. Polym. Sci.*, **28** 1539 (2003).
6. C. Silvestre, D. Duraccio, and S. Cimmio, *Prog. Polym. Sci.*, **36** 1766 (2011).
7. A. Arora and G.W. Padua, *J. Food Sci.*, **75** R43 (2010).
8. C. Johansson. "Bio-nanocomposites for food packaging applications," in Bio-nanocomposites for food packaging applications. Oxford, New York, V. Mittal (2011).
9. J.M. Lagarón and A. López-Rubio, *Trends Foods Sci. Tech.*, **22** 611 (2011).
10. E. Picard, E. Espuche, and R. Fulchiron, *Appl. Clay Sci.*, **53** 58 (2011).
11. D. Sheng, J. Tan, X. Liu, P. Wang, and Y. Yang, *J. Mater. Sci.*, **46** 6508 (2011).
12. A.P. Meera, T.P. Selvin, and T. Sabu, *Polym. Compos.*, **33** 524 (2012).
13. F.J. Rodríguez, A. Torres, A. Peñaloza, H. Sepúlveda, M. J. Galotto, A. Guarda, and J.E. Bruna, *Food Addit. Contam.*, **31** 342 (2014).
14. J.E. Bruna, A. Peñaloza, A. Guarda, F.J. Rodríguez, and M. J. Galotto, *Appl. Clay Sci.*, **58** 79 (2012).
15. D. García-López, J.F. Fernández, J.C. Merino, J. Santarén, and J.M. Pastor, *Compos. Sci. Technol.*, **70** 1429 (2010).
16. A. Somwangthanaroj, K. Photyotin, S. Limpanart, and W. Tanthapanichakoon, *Polym. Plast. Technol. Eng.*, **51** 1173 (2012).

17. J.-W. Rhim, H.-M. Park, and C.-S. Ha, *Prog. Polym. Sci.*, **38** 1629 (2013).
18. J. Ganster and H.-P. Fink. Cellulose and Cellulose Acetate, S. Chichester: Kabasci, (2014).
19. H.-W. Park, M. Misra, L.T. Drzal, and A.K. Mohanty, *Bio-macromolecules*, **5** 2281 (2004).
20. A.K. Mohanty, A. Wibowo, M. Misra, and L.T. Drzal, *Compos. Part A Appl. Sci. Manuf.*, **35** 363 (2004).
21. R. Quintana, O. Persenaire, Y. Lemmouchi, J. Sampson, S. Martin, L. Bonnaud, and P. Dubois, *Polym. Degrad. Stab.*, **98** 1556 (2013).
22. J.A.dL. , C.A. Pinotti, M.I. Felisberti, and M.dC.G. , *J. Appl. Polym. Sci.*, **124** 4628 (2012).
23. J.E. Bruna, M.J. Galotto, A. Guarda, and F.J. Rodríguez, *Carbohydr. Polym.*, **102** 317 (2014).
24. T. Janjarasskul, K. Tananuwong, V. Kongpensook, S. Tantratian, and S. Kokpol, *LWT-Food Sci. Technol.*, **72** 166 (2016).
25. A. Kapetanakou and P. Skandamis, *Curr. Opin. Food Sci.*, **12** 1 (2016).
26. S. Manso, F. Cacho-Nerín, R. Becerril, and C. Nerín, *Food Control*, **30** 370 (2013).
27. D.C. Santos, R. Ribeiro-Santos, L. Ventura, N.R. Melo, B. S. Costa, E.E.G. Rojas, and N.L. Salgado, *Ital. J. Food Sci.*, **28** 248 (2016).
28. Q. Sun, L. Wang, Z. Lu, and Y. Liu, *Int. Biodeterior. Biodegrad.*, **104** 419 (2015).
29. P. Suppakul. "Cinnamaldehyde and Eugenol," in Cinnamaldehyde and Eugenol: Use in Antimicrobial Packaging, J. San Diego, USA, Barros-Velázquez (2016).
30. S. Manso, D. Pezo, R. Gomez-Lus, and C. Nerín, *Food Control*, **45** 101 (2014).
31. M. Balaguer, G. López-Carballo, R. Catalá, and P. Hernández-Muñoz, *Int. J. Food Microbiol.*, **166** 369 (2013).
32. S. Makwana, R. Choudhary, N. Dogra, P. Kohil, and J. Haddock, *LWT-Food Sci. Technol.*, **57** 470 (2014).
33. K. Wattananawinrat, P. Threepopnatkul, and C. Kulsethanchalee, *Energy Procedia*, **56** 1 (2014).
34. M. Wrona, K. Bentayed, and C. Nerín, *Food Control*, **54** 200 (2015).
35. F.J. Rodríguez, L.A. Cortés, A. Guarda, M.J. Galotto, and J. E. Bruna, *J. Mater. Sci.*, **50** 3772 (2015).
36. F.J. Rodríguez, M.J. Galotto, A. Guarda, and J.E. Bruna, *J. Food Eng.*, **110** 262 (2012).
37. V.V. Dighe, A.A. Gursale, and G.A. Charegaonkar, *Chromatographia*, **70** 1759 (2009).
38. ASTM (2013). Standard Method for Determining the Antimicrobial Activity of Immobilized Antimicrobial Agents Under Dynamic Contact Conditions. Vol. **E2149-13**.
39. J. Bandyopadhyay, S.S. Ray, M. Scriba, and J. Wesley-Smith, *Polymer*, **55** 2233 (2014).
40. L. Gall, Messen, Kontrollieren, Rezeptieren. Farbtoleranzen (2009). Resource document. <http://www.farbmeterik-gall.de/cielab/toleranz/index.html>. Accessed 1st. August 2016.
41. W. Xie, Z. Gao, W.-P. Pan, D. Hunter, A. Singh, and R. Vaia, *Chem. Mater.*, **13** 2979 (2001).
42. R.K. Shah and D.R. Paul, *Polymer*, **47** 4075 (2006).
43. K. Stoeffler, P.G. Lafleur, and J. Denault, *Polym. Degrad. Stab.*, **93** 1332 (2008).
44. M.A.D. Nobile, A. Conte, G.G. Buonocore, A.L. Incoronato, A. Massaro, and O. Panza, *J. Food Process Eng.*, **93** 1 (2009).
45. Y. Mystri. Development of LDPE-based antimicrobial films for food packaging. MSc Thesis: Victoria University, (2006).
46. M.J. Galotto, X. Valenzuela, F.J. Rodríguez, J.E. Bruna, and A. Guarda, *Packag Technol Sci*, **25** 363 (2012).
47. P. Suppakul, K. Sonneveld, S.W. Bigger, and J. Miltz, *J. Food Eng.*, **105** 270 (2011).
48. J. Sáez. Development of active eco-nanocomposites of cellulose acetate by extrusion process. Bachelor Dissertation: University of Santiago de Chile, Santiago, Chile, (2012).
49. S. Gemili, A. Yemenicioglu, and S.A. Altinkaya, *J. Food Eng.*, **90** 453 (2009).
50. M. Mastromatteo, G. Barbuzzi, A. Conte, and M.A.D.N. , *Innov Food Sci Emerg*, **10** 222 (2009).
51. S. Kim and M. Rhee, *Food Control*, **60** 447 (2016).
52. J. Puls, S.A. Wilson, and D. Holer, *J Polym Environ*, **19** 152 (2011).